LONDON2007

P098

Far-Field Radiation in Poroelastic Media from a Point Source in a Fluid-Filled Borehole

S.R. Ziatdinov* (St.-Petersburg State University), A.V. Bakulin (Shell International Exploration and Production Inc), B.M. Kashtan (St.-Petersburg State University) & V.N. Troyan (St.-Petersburg State University)

SUMMARY

Cross-well seismic with direct, reflected and tube waves is often used for imaging and monitoring of oil and gas reservoirs. Even though downhole sources are usually located in the borehole fluid, at low frequencies their radiation is modified by the presence of poroelastic formations surrounding the well. Permeable formations also enhance the conversion of borehole tube waves into body or other formation waves, which is an important foundation for a tube-wave monitoring. To capture the influence of porous and permeable formation on radiation of formation waves, we derive analytic expressions for a far-field radiation of compressional and shear waves from a point pressure source located inside a fluid-filled borehole. We demonstrate how various attributes of this radiation are controlled by permeability and viscosity of the pore fluid and other parameters at low seismic frequencies. We show that radiation patterns in formations with good permeability can be distinguished from the radiation patterns in an equivalent elastic impermeable media. To verify obtained results we compare analytical far-field radiation with a finite-difference computations and observe good agreement between the two approaches.

Introduction

Cross-well seismic is widely used for imaging and monitoring of oil and gas reservoirs. The solution for the wavefield excited by a source in the borehole surrounded by the isotropic elastic media was derived by Biot (1952) and Krauklis (1976). The problem of evaluating the far field outside the borehole surrounded by elastic media was presented by Lee and Balch (1982). In this study we focus on a task of cylindrical borehole surrounded by homogeneous poroelastic Biot media. This task is important for cross-well tube-wave monitoring which relies on increased conversion of tube waves into body and guided waves on poroelastic layers compared to elastic impermeable beds (Korneev et al, 2006). Such conversion can be thought as a secondary point source in the borehole and we aim to understand how presence of permeable porous formation modifies the radiation. We present a low-frequency approximation to the full wavefield in the far zone using repeated Fourier and Fourier-Bessel contour integrals and method of steepest descent. We only consider case of "fast formation" when tube-wave velocity is less then the formation shear velocity. In particular, we obtain asymptotic representation for the far-field radiation of of shear, fast and slow compressional body waves.

Theory

Let us consider a fluid-filled borehole $r < r_b$, surrounded by the infinite porous media $r > r_b$. Borehole fluid is characterized by acoustic velocity V_{bf} and density ρ_{bf}. The porous media is characterized by three velocities V_+, V_- and V_S for fast compressional, slow compressional and shear waves respectively. Point pressure source is located on the borehole axis. Boundary conditions on the wall of the borehole consist of continuity of normal stress, radial displacement, continuity of fluid pressure between a borehole fluid and pore fluid, and vanishing of shear stress. Following Chang et al. (1988), these can be represented as a set of four linear equations: M**A**=**B**, where M is 4x4 matrix containing components of stress tensor and displacements on the borehole wall, **A** is a vector of unknown amplitude coefficients for the reflected wave in the borehole fluid and transmitted waves inside the porous media, **B** describes the source terms.

To estimate the far-field radiation at point R (Fig. 1) we should solve for amplitude coefficients **A**. They are obtained by simplifying the linear equations with low-frequency approximation and applying Cramer's rule. After substituting formulae for **A,** approximating Hankel functions for $\omega r >> 1$ in the integral solution, and using method of steepest descent, we derive frequency-domain expressions for the skeleton displacement (U_R, U_θ) in the porous media, in which we retain only terms that decay as $\frac{1}{R}$:

$$U_R(\omega,R,\theta)=[\frac{(2\zeta_+^2\cos^2(\theta)-\zeta_S^2)}{N\zeta_S^2W_+}-\frac{2\phi H_1^{(1)}(\omega\zeta_{r-p1}r_b)}{r_b\Pi_{p1}W_+}]\frac{i\omega e^{i\omega\frac{R}{V_+}}}{RV_+}+[\frac{4i\phi}{\pi r_b^2\Pi_{p2}W_-}]\frac{i\omega e^{i\omega\frac{R}{V_-}}}{RV_-}\quad,\qquad(1)$$

$$U_\theta(\omega,R,\theta)=-[\frac{i\sin(2\theta)}{NW_S}]\frac{i\omega e^{i\omega\frac{R}{V_S}}}{RV_S}\quad,\qquad(2)$$

where Q, G_-, K_{bf}, κ, η are parameters defined in the same way as in Chang et al (1988), T is identical to R defined in Chang et al (1988), $\zeta_\pm=\frac{1}{V_\pm}$, $\zeta_S=\frac{1}{V_S}$, $\zeta_b=\frac{1}{V_{bf}}$, $\zeta_{r-p1}=\sqrt{\zeta_-^2-\zeta_+^2\cos^2(\theta)}$, $\zeta_{r-p2}=\zeta_-\sin(\theta)$, $\zeta_{r-S}=\sqrt{\zeta_-^2-\zeta_S^2\cos^2(\theta)}$, $W_k=\frac{\zeta_k^2\cos^2(\theta)}{K_{bf}\zeta_b^2}-\frac{1}{N}-\frac{1}{K_{bf}}+\frac{2\kappa\zeta_{r-k}H_1^{(1)}(\omega\zeta_{r-k}r_b)}{i\eta r_bH_0^{(1)}(\omega\zeta_{r-k}r_b)}$, where k = +, –, s; $\Pi_j=(G_-T+Q)\omega^2\zeta_-^2H_0^{(1)}(\omega\zeta_{r-j}r_b)$, where *j=p1, p2*. It is clear from the symmetry of the

problem and approximation that U_R contains only compressional, whereas U_θ contains only shear-wave radiation. Indeed the first exponential term of U_R containing V_+ corresponds to the fast compressional wave, whereas second terms with the exponent contaning V_- describes radiation due to slow compressional wave. Tangential displacement U_θ depends only on V_S and describes far-field radiation of shear wave.

Radiation pattern

Let us examine numerically the far-field radiation from a fluid-filled borehole surrounded by poroelastic media. Parameters of porous are given in Table 1 whereas fluid (water) has bulk modulus K_{bf} = 2.2 GPa and density ρ_{bf} = 1000 kg/m^3. The radius of the borehole r_b is 0.1 m. Equations (1) and (2) describe radiation pattern (U_R, U_θ) in the far field and can be plotted as a function of the polar angle θ. For frequencies much lower than critical Biot frequency the second term in U_R that is responsible for the displacement of slow compressional wave is several orders of magnitude smaller than other terms corresponding to the fast compressional wave in U_R and shear wave in U_θ and we do not plot it.

Table 1. Parameters of poroelastic media [notations are as in Change et al (1988)]

Parameters	**Values**	**Parameter**	**Values**
Grain modulus K_s	33.4 GPa	Fluid density ρ_f	1000 kg/m^3
Pore fluid modulus K_f	2.25 GPa	Grain density ρ_s	2650 kg/m^3
Frame bulk modulus K_b	7.03 GPa	Permeability κ	0.3 Darcy
Shear modulus N	4.91 GPa	Porosity φ	0.21
Tortuosity α	2.1	Viscosity η	0.01 Poise

Let us compare far-field radiations for the poroelastic media and equivalent elastic media. We assume that equivalent elastic media has the same P- and S-wave velocities as a low-frequency values of fast compressional and shear velocities for poroelastic media. We plot all radiation patterns for fixed seismic frequency of 100 Hz that corresponds to low-frequency regime $\omega << \omega_b$ (critical Biot frequency f_b is 106 kHz). Since wavefield only depends on the ratio of permeability and viscosity it is convenient to introduce $m = \kappa/\eta$ and call it mobility. For the poroelastic media at hand mobility m is 300 md/cp.

Figure 2 shows radiation pattern for the fluid-filled borehole surrounded by the porous media. Maximum amplitude of a shear wave is radiated in direction of θ = 33.5° while amplitude of the fast compressional wave is strongest in a direction perpendicular to the borehole. Ratio of peak shear (A_s) and compressional (A_p) amplitudes is equal to A_s/A_p=1.51.

Let us consider effect of various poroelastic parameters on the radiation patterns. First, let us examine effect of lowering the mobility of poroelastic media which brings it closer to the impermeable elastic media (m=0). In a first case we decrease mobility by a factor of 100 to m = 3 md/cp, which leads to Biot frequency increase to f_b = 10.6 MHz. Then radiation patterns (Fig. 3) for poroelastic media approach those for elastic media: maximum amplitude of shear wave is emitted in the direction of θ = 30° (in elastic case θ = 30°); ratio of peak amplitudes also converges closer to elastic impermeable limit A_s/A_p=1.82 (in elastic case A_s/A_p=1.86). Peak of the compressional arrival still propagates perpendicular to the borehole. Overall we can conclude that decreasing mobility (increasing viscosity or decreasing permeability) makes the poroelastic medium to appear "closer" to impermeable elastic media and it is reflected in the behavior of radiation patterns.

Now let us examine effects of elevated mobility. Let us increase mobility by a factor of 33 to m = 10^4 md/cp which can be done by either viscosity decrease ($\eta = 3*10^{-4}$ Poise) or permeability increase (κ=10 Darcy). This will diminish Biot frequency down to f_b = 3.2 kHz, but we still remain at low frequency regime. In this case shear wave with peak amplitude propagates in the direction of θ = 37.5° and relation A_s/A_p decreases to 1.33. These values deviate further from the elastic media making radiation patterns more distinct between porous and equivalent elastic media. We may also interpret decrease of A_s/A_p in a porous media with

higher mobility as redistribution of elastic energy from shear to fast compressional wave. Finally, different radiation in elastic and poroelastic media can shed some light on why tube-wave conversion to body and guided waves is larger on permeable as opposed to impermeable layers (Korneev et al., 2006).

Finally, let us examine the influence of the borehole fluid on the radiation pattern. Let us reduce bulk modulus of borehole fluid from K_{bf} = 2.2 GPa to K_{bf} = 1.8 GPa (Fig. 4). While absolute amplitudes of the far-field radiation amplitudes do change for both porous and elastic media, the directions of peak shear and compressional amplitudes remain fixed. However ratio A_s/A_p for elastic media decreases by 15%, whereas for porous media it only drops by 6%. We conclude that the change in borehole fluid parameters has greater influence on energy distribution between shear and compressional waves in case of elastic media.

Comparison with finite-difference computations

To verify obtained analytical expressions for far-field radiation we compare the predicted amplitudes with those obtained from finite-difference computations for the same model of a borehole surrounded by a homogeneous poroelastic formation as in a previous section (m = 300 md/cp). Figure 5 shows snapshots of the total vector of displacement velocity for the skeleton ($\sqrt{U_r^2 + U_z^2}$). Fast compressional wave has peak amplitude in the direction perpendicular to the borehole axis (Fig. 5a). Figure 5b shows that maximum amplitude along the shear-wave front occurs at $\theta = 33.5°$ and $\theta = 146.5°$ as predicted by analytic solution for far-field radiation. In both cases we observe good agreement between finite-difference waveforms and derived analytical expressions for the far-field P- and S-wave radiation.

Conclusions

We obtained a low-frequency approximation for the far-field radiation of compressional and shear waves in the surrounding porous media from a point pressure source in a fluid-filled borehole. Recording fast P-wave and S-wave radiation one can distinguish poroelastic and elastic media by utilizing two attributes: ratio of peak amplitude of P- and S-waves and direction of the peak shear amplitude. Obtained radiation patterns approach those for equivalent (defined as having the same velocities) elastic media when parameters of the porous media become "closer" to elastic impermeable formation. For instance, when mobility is 300 md/cp, then radiation patterns of elastic and poroelastic media can be distinguished. However when mobility decreases to 3 md/cp, they become almost indistinguishable. When mobility becomes very large (~ 10^4 md/cp) then abovementioned attributes in porous case deviate even further from elastic media: A_s/A_p ratio decreases, whereas angle of maximum shear amplitude increases. Obtained far-field radiation is in good agreement with finite-difference computations which confirms accuracy of obtained analytical expressions.

References

Biot, M.A. [1952] Propagation of elastic waves in a cylindrical bore containing a fluid. J. Appl. Phys. 23, 997-1005.

Korneev, V., Bakulin, A., and Ziatdinov, S. [2006] Tube-wave monitoring of oil fields. 76th Meeting, Society of Exploration Geophysicists, Expanded Abstract, 374-378.

Krauklis, P.V., Krauklis, L.A. [1976] Wave field of point source in the borehole. Dynamic Theory of Seismic Wave Propagation. 16, 41-53 (in Russian).

Lee M. W., Balch A.H. [1982] Theoretical seismic wave radiation from a fluid-filled borehole. Geophysics 47, 1308-1314.

Chang S.K., Liu H.L., and Johnson D.L. [1988] Low-frequency tube waves in permeable rocks. Geophysics 53, 519-527.

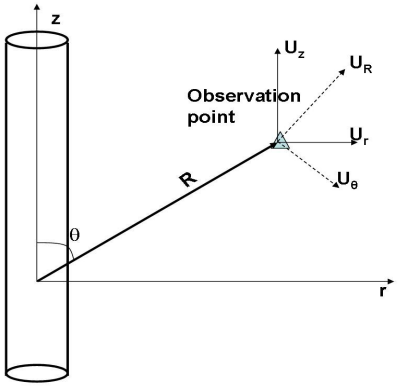

Figure 1. Model of a borehole surrounded by poroelastic media. While the problem is solved in cylindrical coordinates (U_r and U_z), the far-field radiation for matrix displacement is more convenient to represent in spherical coordinates (U_R and U_θ).

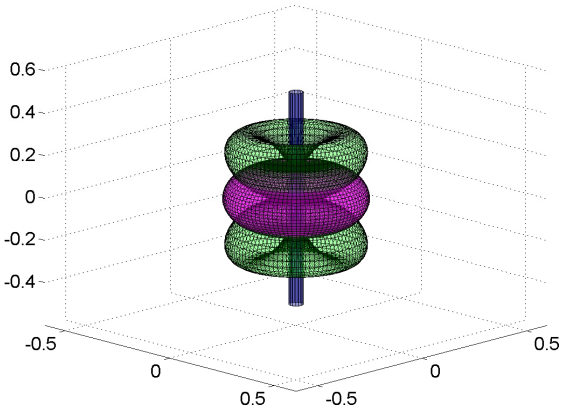

Figure 2. Radiation pattern of the fast compressional wave (magenta) and shear wave (green) when mobility m = 300 md/cp.

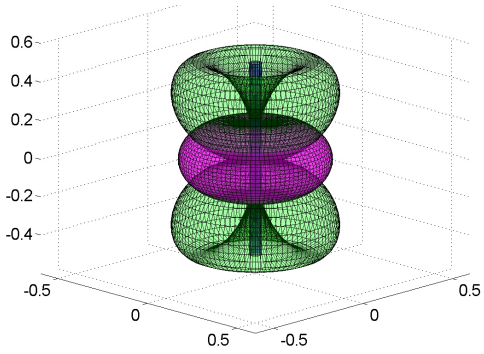

Figure 3. Radiation pattern of the fast longitudinal wave (magenta) and shear wave (green) when mobility decreases to m = 3 md/cp.

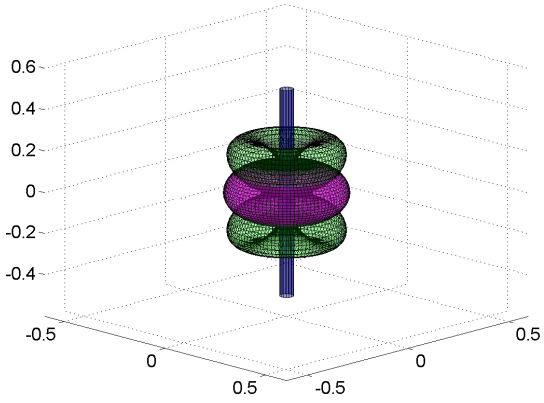

Figure 4. Radiation patterns of the fast longitudinal wave (magenta) and shear wave (green). Parameters are as in Table 1 except that bulk modulus in the borehole is K_{bf} = 1.8 GPa.

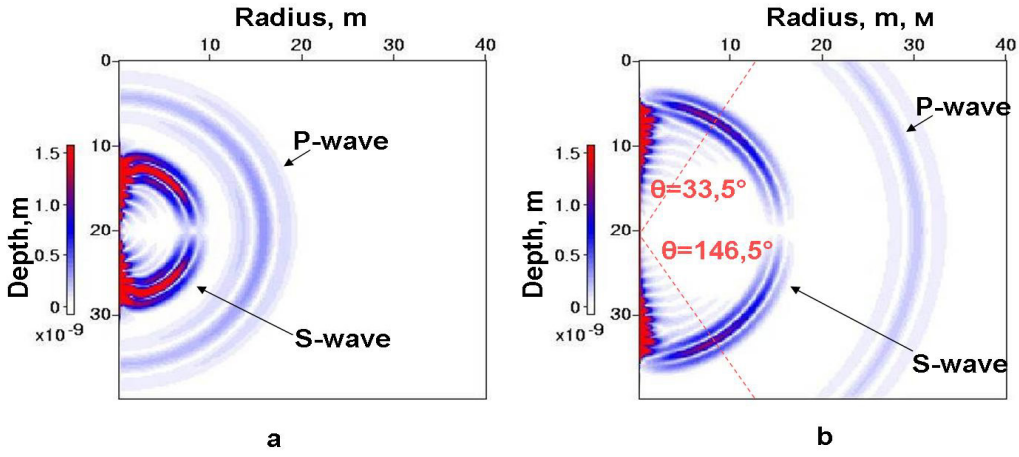

Figure 5. Snapshots of the total vector of matrix velocity ($\sqrt{U_r^2 + U_z^2}$) obtained with a finite-difference code for a wavelet with a 100 Hz central frequency: (a) at time t=7.5 ms , (b) at time t=12 ms.